

To the 70-th Anniversary of Marin Ivaşcu

RELIABLE SOFTWARE IN COMPUTATIONAL PHYSICS

GH. ADAM*, S. ADAM†

Department of Theoretical Physics

*National Institute of Physics and Nuclear Engineering "Horia Hulubei",
IFIN-HH, P. O. Box MG-6, R-76900 Bucharest-Măgurele, Romania*

Abstract

A bird's-eye-view of the approach offered by the computational physics to the solution of the problems of physics is given with emphasis on the key issue of reliability. Some meanings of the reliability are illustrated by specific examples.

Keywords: Physical model; Data processing; Algorithm; Program; Software; Process; Hardware; Input; Output; Insight; Reliability; Positron Spectroscopy; Fermi surface; High- T_c superconductivity; Quadrature.

1 INTRODUCTION

The field of computational physics is at the interface between the theoretical and/or experimental physics, numerical analysis, and computer science. Theoretical physics provides models to the investigated physical phenomena, experimental physics provides large sets of raw data needing signal processing to extract the desired useful information, numerical analysis provides mathematical methods leading to meaningful algorithms for the solution of the models of the investigated phenomena or pertaining to data analysis, while computer science provides a wealth of structures devised for efficient use of the hardware at hand. The use of computers enabled the study of intricate physical phenomena that could not be reduced to simple analytically soluble models.

*Corresponding author; e-mail: adamg@theory.nipne.ro

†e-mail: adams@theory.nipne.ro

It is worthwhile to observe that the computer based research done in physics always involved a large fraction of ephemeral efforts stemming from both the to-date status of the available hardware and software and their grasp. On one side, the availability of facilities drastically limited the purpose and scope of the research effort done by a certain group. On the other side, the rapid pace of the hardware and software development, while allowing considerable extension of the scale of the research projects, was hindered by the strenuous effort required from behalf the individuals to grasp the capabilities of the newly added facilities.

However, during the half century history of the computational physics, there has been accumulated a steady ground which deserves attention. In this paper, we address three main topics: the general frame of a research project involving computational physics (section 2), the reliability as the key concept towards insight from the input at hand (section 3), and specific illustrations of reliability (section 4).

2 STEPS OF COMPUTER BASED RESEARCH

The starting point (the **input**) of a research project involving computational physics is a certain **physical model** intended to describe theoretically either a physical **phenomenon** or a set of **data** collected during an experiment. The characteristic feature of such models is a *high intrinsic complexity* which results in the fact that the underlying mathematical models do not admit closed form calculable analytical solutions, such that recourse is to be made to computing.

The obtained *primary* numerical **output** usually consists of a set of a great many *numbers* the meaning of which can be grasped only after some **secondary processing** using a kind or another of *visualization graphics* [1].

The flowchart in fig. 1 illustrates the occurrence of two kinds of flows of information established during the advancement from the input to the output: a *direct* (feed before) and an *inverse* (feed back) flow.

The direct flow (shown in thick solid line arrows) illustrates the necessary steps to be done by a successful project. There are three main distinct steps along the direct flow: the algorithm, the program, and the process.

The inverse flow describes the *control* which is compulsory in order to secure the consistency of the whole process. The **insight**, shown as the distinct final step in fig. 1, is the term which might adequately characterize all the feed back paths (starred line arrows in fig. 1). The main features of these four steps are briefly characterized in the next subsections.

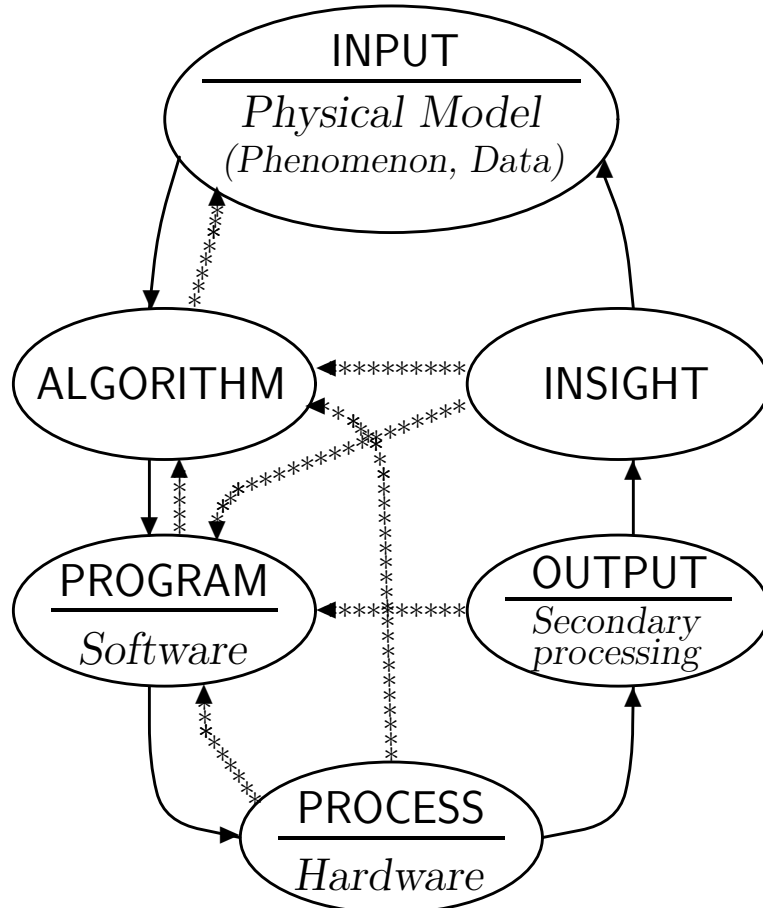


Figure 1: Cycle of a research project involving computational physics.

2.1 THE ALGORITHM

- Approximates the actual solution S of the input problem by a couple (s, e) , in a finite number of primitive mathematical operations where:
 - s denotes the approximate solution (easy task)
 - e denotes the error associated to s (hard task).
- Intrinsic feature: complexity – estimates how **large** the finite number of principal high-level symbolic primitives is (deep understanding of input may result in **significant reduction of complexity**). Complexity points to problem solvability.
- Algorithm formulation uses the language of *algebra* (hence the group algebraic properties of commutativity, associativity, distributivity, etc.,

result in classes of equivalent algorithms).

- **Feed back features.** The assessment of complexity is necessary to establish the best approach to the solution. Often, the data analysis needs the formulation of criteria addressing the control of the input consistency/correctness.

2.2 THE PROGRAM

- Expresses the algorithm in a form understandable (*after processing*) by the hardware.

The processing expresses a set of analysis/translation operations which convert the high level abstract primitives of the source program into primitive algebraic operations of the assembly language.

- The program formulation by use of high level abstract primitives is possible within one of the four existing programming paradigms [2]: **procedural** (e.g., Fortran 77, Fortran 95, C, Pascal, Ada), **functional** (e.g., Lisp), **object oriented** (e.g., Ada 95, C++, Java), or **declarative** (e.g., Prolog).

During the eighties, the mainstream of the algorithm programming in computational physics was based on the use of Fortran 77, which secured the fastest running speed. However, the lack of available cheap Fortran 95 compilers and the standardization of C++ accompanied by the availability of free compilers has shown, during the last decade, a steady shift of interest toward this programming language.

- The program shows specific **language dependence** concerning:
 - Available symbolic *primitives*,
 - Language *conventions* for complex data storage, the observation of which increases **efficiency**,
 - Memory allocation: static/dynamic,
 - Recursivity.
- **Feed back feature:**
 - Efficient memory programming induces specific algorithmic structures: vectors, lists (queues, stacks), trees, etc.

2.3 THE PROCESS

- Denotes the chain of central processing unit (CPU) elementary operations resulting in the algorithm advancement from the input data to the output.

• Features governed by <i>hardware architecture</i>	\implies • Feed back features
– Quantization (discretization) of floating point numbers	– Search for a <i>stable path</i> with respect to roundoff noise propagation – Break down of the algebraic algorithm equivalence
– Hierarchical memory organization Processor(s) \Rightarrow \Rightarrow Cache(s) \Rightarrow \Rightarrow (S/D)RAM \Rightarrow \Rightarrow HDD	– <i>Principle of locality</i> asks for <i>static</i> memory allocation <i>Multitasking</i> asks for <i>dynamic</i> memory allocation <i>Reconciliation: granular</i> memory allocation [3]
– <i>One processor vs</i> <i>multiprocessor</i> architecture	– <i>Sequential vs</i> <i>parallel (distributed)</i> algorithm formulation

2.4 THE INSIGHT

”*Computing is insight, not numbers*”, the illuminating motto which opens the famous monograph by Richard Hamming [4] sums up the deep understanding of computing. On one side, there is a *gradually distributed* insight along the research cycle. Each of the three main steps, the algorithm, the program, and the process, brings *specific insights* (broken arrows in fig. 1) which validate the respective steps and allow reliable advancement towards the final answer.

On the other side, there is the *final insight* step shown in fig. 1, the meaning of which is threefold. The pointers (in broken arrows) towards the program and the algorithm show the completion of *inner cycles* of the research effort, which may result in the development of new specific research tools able to solve the current problem or a larger class of problems.

The solid insight arrow pointing to the physical model in fig. 1 ends the research cycle for the investigated model. This insight is always a challenge. Without proper valuation of the quests concerning the algorithm and the program, the conclusions addressing the physical model may be deprived of significance. Why this might happen can be understood in a simple way. The automatic decisions implemented in the so-called class conscious algorithms allowed decision tailoring in terms of the actual features of the currently solved problem. However, each of the decision branches implemented in such a program is based on the assumption that the *heuristics* underlying the derivation of an estimate to the accuracy e of the approximate result s holds true. The use of the existing software libraries to solve new problems in

contexts which are *different* from those taken into account at the elaboration of the programs is thus a very sensible point which has to be considered with the greatest care.

3 SOFTWARE RELIABILITY

The quality characteristics of a code, established by Boehm et al. a quarter of century ago [5], include several important features such as reliability, robustness, efficiency, user friendliness, modular organization, and portability.

The development of good programming practices has been accompanied by efforts to include the software qualities into the high level programming languages, with the aim to guide the user as closely as possible into problem adapted efficient structured thinking, the elaboration of machine independent programs unveiling at a glance the programmer's intentions, the rejection of obviously inappropriate input.

The reliability, which designates the ability of the program to yield trustful outputs for all possible significant inputs, deserves special consideration. Of course, the programming mistakes result in trivially unreliable output. Their removal from a program is programmer's responsibility and is outside the scope of the present discussion.

We notice first the existence of reliability features which *could* be incorporated in structured programming languages (like, e.g., modular implementation, reliable data transfer to and from procedures, data abstraction allowing right correspondences between the various quantities within complex problems). There are, however, reliability requirements which cannot be solved by improving the design of the programming languages.

An important source of software unreliability comes from the fundamental difference which differentiates an algorithm from a related mathematical method. While a mathematical method can reach the right answer within an *infinite* number of elementary algebraic operations, the algorithm involves, by its very definition, a *finite* number of operations only, hence it cannot check the fulfillment of the conditions ensuring the validity of rigorous mathematical results implicitly or explicitly based on the process of passing to the limit.

As a consequence, much of the effort to ensure reliability is devoted to the derivation of consistency conditions relating a given algorithm to its underlying mathematical method. Such an effort is hence specific to the branch of the numerical analysis involved in the algorithm design. The following discussion considers a few relevant examples encountered in computational physics.

A great many problems involving floating point computation ask for *the control of the roundoff generated noise*:

- In the solution of ordinary differential equations, the condition of *convergence* of the discrete numerical solution to the continuum solution is necessary, but not sufficient. The reason is that the roundoff noise may induce *spurious* solutions which get *enhanced* under solution propagation to the neighbouring knots. A numerical solution reaches the continuum solution provided it is *stable*, i.e., the roundoff noise generated in the computed data (associating spurious solutions) at a certain space or time coordinate within a mesh gets *damped* under solution propagation to the neighbouring mesh coordinates. The study of the conditions under which this requirement can be fulfilled resulted in several forms of stability criteria which have to be satisfied by the coefficients of the differential equations belonging to specific classes.
- If the algorithm gets the solution via recurrence relations, the problem is to find *stable paths* along which the roundoff error propagation gets damped, in contradistinction to the opposite sense of the recurrence relation along which the roundoff errors are enhanced exponentially. In the most favourable case, the recurrence is stable either in the forward sense or the backward one. However, it might happen that a mixture of the two recurrence senses secures accurate propagation of the solution.
- The matrix inversion, which is a key operation for many linear algebra algorithms, is very sensitive to the *matrix conditioning*, measured by the magnitude of the spectral radius of its spectrum. This is the fundamental parameter controlling the numerical accuracy of such an operation.
- In the numerical solution of linear systems, one way of securing better conditioning properties of the matrix coefficients is the transformation of the system into an algebraically equivalent form which is characterized by a coefficient matrix with a lower condition number.

A correct algorithm reaches the right solution in the *continuum limit* $n \rightarrow \infty$ of the discrete mesh used to solve the problem. The numerical quadrature provides instances where this natural condition is not automatically satisfied.

In the case of Newton-Cotes quadrature, the intuitive reason for this ill-behaviour is the occurrence of *cancellation by subtraction*, originating in alternate sign dependence quadrature weights at adjacent quadrature knots, such that the absolute magnitudes of the quadrature weights increase with n .

In the case of the Chebyshev quadrature, it simply happens that the condition to get quadrature sums characterized by equal to each other quadrature weights does not result in real solutions at $n > 8$.

A more subtle unreliable result is provided by the Gauss quadrature sums. Here the intrinsic properties of the basis Legendre polynomials spanning the approximating space of the n -th degree interpolatory polynomial result in the property that, while coinciding with the true integrand at the quadrature knots, the deviations of this polynomial from the true integrand *inbetween the quadrature knots* may become infinitely large as $n \rightarrow \infty$.

In contradistinction to these, the Clenshaw-Curtis quadrature reaches the right result in the limit $n \rightarrow \infty$ with an interpolatory polynomial uniformly converging towards the integrand values everywhere inside the integration domain.

A *quadrature rule* provides both terms of the pair (s, e) mentioned in section 2.1. Using a carefully selected set of quadrature rules, the automatic adaptive quadrature tailors the subrange discretization to the integrand behaviour over the integration domain. Adding some specific convergence acceleration techniques, the automatic adaptive quadrature extends the use of the quadrature rules to the efficient solution of both proper and improper Riemann integrals. This is done by means of automatic decisions concerning the algorithm branch to be followed in terms of the specific integrand behaviour detected during the subrange subdivision refinement.

This approach offers still another kind of unreliability: during the problem solving process, the choice of the appropriate integrand dependent branch is based on some *heuristic hypothesis* rather than upon the fulfillment of the theorematic results guaranteeing the reliability of the decision. It may thus happen that an insufficiently resolved integrand profile spuriously points towards a condition enabling the activation of a convergence acceleration algorithm. From this point on, everything is lost: the departure of the computed result from the actual one may be arbitrarily large, while the routine ends the automatic quadrature process with an error estimate e within the input accuracy specifications, hence the diagnostic of safe output!

A final example concerns the signal processing of experimental data characterized by a small signal to noise ratio. Then everything becomes questionable and has to be carefully considered into the analysis algorithm: the relationship between the laboratory frame and the theoretical frame where a physical model is usually developed in the absence of noise, and the investigation of the possibility to define resonant-like functions able to result in a reliable reference frame; the nature of the on-line data discretization; the definition of fixed points of the spectrum showing well characterized stability

basins; removal of the background contribution to the measured spectrum.

In conclusion, reliability shows features the fulfillment or failure of which is entirely under the control of the creator of the program.

4 ILLUSTRATIVE EXAMPLES

In this section, we illustrate several aspects of the reliability with examples originating in projects of computational physics in which we have been directly involved:

- (i) *Study of physical properties of transition metals* [6];
- (ii) *Signal processing in 2D-ACAR positron spectroscopy* [7]-[13];
- (iii) *Class conscious integration* [14], a topics resumed at the end of the nineties [15], [16];
- (iv) *Perturbative numerical methods for the solution of ordinary differential equations* [17];
- (v) *Crystalline electric fields and giant magnetic anisotropy in rare earth intermetallics* [18], [19];
- (vi) *Channeling radiation of energetic charged particles in crystals* [20], [21];
- (vii) Study of the *two band singlet-hole Hubbard model* developed by Plakida [22] with the aim to elucidate the *mechanisms of the high- T_c superconductivity in cuprates* [23].

Among these topics, those labeled (i), (ii), (v), (vi), and (vii) dealt with concrete physics problems the solution of which had to run through all the stages shown in fig.1.

The topics (iii) and (iv) addressed well defined subjects in numerical analysis the solution of which provided tools for the numerical investigation of specific problems of physics. Thus, the software developed for the solution of Sturm-Liouville problems (topics (iv)) served to the computation of the first dipolar harmonics of the planar channeling radiation of the ultra-relativistic positrons (topics (vi)). The computation of parametric integrals (topics (vii)) showed that the existing quadrature rules (topics (iii)) are inadequate and an effort in this direction was started [24].

In the sequel, ways of achieving reliable solutions are illustrated for some of these problems.

4.1 DATA ANALYSIS IN POSITRON SPECTROSCOPY

In this subsection, the identification of the Fermi surface sheets in high- T_c superconducting single crystals from positron spectroscopy data is reviewed. The experimental setup collects n -axis-projected histograms by the technique of two-dimensional angular correlation of the electron-positron annihilation radiation (2D-ACAR) coming from zero-spin positron-electron pairs [25],[26].

Reliable signal processing is done provided three distinct problems are solved: (i) appropriate characterization of the main features of a 2D-ACAR histogram, (ii) data reformulation from the laboratory frame to the crystal frame, and (iii) statistical noise smoothing and background removal.

4.1.1 The main features of the 2D-ACAR histograms

1. The initial stages of the positron interaction with the lattice of a high- T_c single crystal proceed similarly to those in normal metals. Before annihilation, the positrons reach thermal (or nearly thermal) equilibrium with the lattice and get spatially distributed along a characteristic “implantation profile”, which is sufficiently deep such that the greatest fraction of the thermalized positrons annihilates in the bulk of the sample under study. Because of the strong Coulomb interaction of the positrons with electrons and ions, and as a consequence of the lamellar structure of the crystalline high- T_c superconductors, two features of the 2D-ACAR technique are to be noted: (a) the “positron energy band” formed by the low-energy positron states induces specific *positron wavefunction effects* in the measured histograms, which have to be dropped off from the output of the signal analysis; (b) the usefulness of the method is limited to the resolution of electronic Fermi surface sheets, extending over the crystal regions which attract the positrons.
2. The transverse momentum distribution inside the 2D-ACAR histogram plane can be split into *Umklapp components*, which are related to the n -axis-projection of the first Brillouin zone (1BZ) of the sample in the *extended zone representation*, with an amplitude of the useful signal that rapidly decays towards the higher Umklapp components. Let

$$\{D_M | M = 0, 1, \dots, M_{max}\}. \quad (1)$$

denote the areas centred at Γ_{00} , the *zero momentum projection of the centre Γ of 1BZ onto the histogram plane*, and covering the first M -Umklapp components inside the histogram plane. The edges of D_0 are then respectively given by appropriate projections, $\{p_x, p_y\}$, of the

primitive translation vectors of the reciprocal crystal lattice onto the histogram plane. The edges of D_M ($M \geq 1$) are given respectively by $\{(2M+1)p_x, (2M+1)p_y\}$. Thus, D_M consists of a collection of regions of areas D_0 , centred at histogram points Γ_{mn} of coordinates

$$p_x^{(m)} = mp_x; p_y^{(n)} = np_y; m, n \in \{-M, \dots, M\}. \quad (2)$$

The number M_{max} of the Umklapp components available within a particular 2D-ACAR histogram is defined by the geometry of the experiment and the angular aperture of the setup. Usually, $M_{max} = 2$ [27] or 3 [10].

3. The positron annihilations contributing to the measured 2D-ACAR signal occur at electrons within bands crossing the Fermi level, at bound electrons, and at electrons at crystal inhomogeneities. Artifacts also give an important contribution to the histogram bins.

The fraction which originates in the conduction electrons will show a quasi-periodic distribution over the histogram plane, with symmetries of the transverse momentum spectrum around the points Γ_{mn} , Eq. (2), as emerging from the subduction to the histogram plane of the symmetry properties of the electron energy bands of the crystal in the extended zone representation. In high- T_c superconductors, the magnitude of this *useful* fraction of the momentum distribution does not exceed a few percent of the accumulated statistics [28] and this is the main reason why giga-count statistics is needed to get well-resolved Fermi surface sheets [27].

The fraction which originates in the bound electrons will show a unique symmetry centre, Γ_{00} , with an overwhelming radially symmetric component and a localized component defined by the symmetry of the energy band crystal field splittings.

The fraction which originates in electrons at crystal imperfections is responsible for the enhanced spectral intensities of the experimental data at low momenta in comparison with theoretical data calculated under the assumption of perfect crystalline periodicity [7, 29, 30]. Similar to the previous fraction, there is a unique symmetry centre of it, Γ_{00} , with an overwhelming radially symmetric component [30].

While the systematic instrumental artifacts are ruled out by specific procedures [10], there still remain residual artifacts the distribution and magnitude of which are unknown. The occurrence of *zero mean randomly distributed residual artifacts* represents the most favorable hypothesis on the quality of the 2D-ACAR histogram under analysis. If,

however, the artifacts have their own centre, different from Γ_{00} , then the computed centre of the 2D-ACAR distribution will be pulled away from Γ_{00} [31]. As a consequence, the off-line data processing has to include criteria proving that the magnitude and distribution of the artifacts will have a negligibly small effect on the inferences of the data analysis.

4. Within a 2D-ACAR experiment, the data is *discretized* in square bins of side a_D defined by the detectors and the geometry of the setup. In what follows, if not specified otherwise, the in-plane coordinates and lengths are given in discretization step units a_D . The bins are then labeled by pairs of integers, (i, j) , which correspond to the bin centres inside *the detector defined histogram plane*, $Op_x^D p_y^D$. As shown in detail in [10], this discretization defines a *piecewise constant continuous* momentum distribution over the histogram plane.
5. Within each histogram bin, the counts obey a Poisson statistics.

4.1.2 Data redefinition from laboratory frame to crystal frame

Essential for the success of the signal analysis is the operation of *histogram redefinition from the laboratory frame (LF)*, $Op_x^D p_y^D p_z^D$, (defined by the setup and within which the data acquisition is performed) *to the crystal frame (CF)* $\Gamma_{00} p_x p_y p_z$ (identified with the projection of the canonical reference frame of the 1BZ along the n -axis and within which the various steps of the off-line analysis of the spectrum are legitimate). An n -axis-projected 2D-ACAR spectrum is secured by tuning the crystal axes to the detector axes. Under perfect tuning, the LF axis Op_z^D , normal at O to the histogram plane $Op_x^D p_y^D$, and the CF axis $\Gamma_{00} p_z$, are parallel to each other. Within data analysis, this condition is assumed to be fulfilled provided the Euler angle θ_0 , Eq. (4), relating the CF to LF is negligibly small.

Thus, a consistent off-line analysis has to begin with the definition, if at all possible, of the CF and then to continue with the reformulation and processing of the 2D-ACAR histogram in this frame, under close scrutiny of the magnitude of the departures of the histogram features from the ideal ones.

Since the positron annihilation technique is non resonant, the derivation of the crystal frame from the LF data is to be done by a mathematical procedure able to maximize the *characteristic symmetry pattern* induced in a 2D-ACAR histogram by the occurrence of the Fermi surface, while minimizing the other contributions listed in Sec. 4.1.1, item #3. The concept of *signature of crystal symmetry (SCS)* in a 2D-ACAR histogram [11, 12], fulfills this

requirement.

The SCS of interest for signal analysis is defined both for the raw histogram $H = (h_{pq})$ and for the histogram $S = (s_{pq})$ obtained from H by a procedure of statistical noise smoothing *which does not involve symmetrization* (Sec. 4.1.3). It consists of a set of chi-square *densities per bin* which measure the goodness of the assumption that some suitable (κ, λ) sites inside the histogram plane $Op_x^D p_y^D$ can be taken for Γ_{00} . For single crystals of orthorhombic symmetry, admissible (κ, λ) sites are *bin centres*, *bin corners* and *centres of bin sides*, inside a convenient neighbourhood of the centre O of H .

For the histogram H , the SCS elements are chi-square sums

$$\chi_0^2(\kappa, \lambda; \widetilde{D}_M; H) = \frac{1}{N_M} \sum_{(i,j) \in \widetilde{D}_M} \sum_{(k,l) \in (i,j)^*} (h_{ij} - h_{kl})^2 / \sigma_{ij}^2. \quad (3)$$

Here, the summation region \widetilde{D}_M , centred at (κ, λ) , denotes the closest *entire bin approximation* of the M -Umklapp area (1). The notation $(i, j)^*$ denotes the manifold of histogram bins which can be obtained from the (i, j) -th bin by point group symmetry operations. The quantity σ_{ij} is estimated taking into account Sec. 4.1.1, item #5. Finally, the normalization factor N_M equates the total number of symmetry defined pairs of distinct bins inside \widetilde{D}_M .

For a 2D-ACAR histogram characterized by zero mean randomly distributed residual artifacts, the $M_{max} + 1$ obtained SCS sets would result in a *same set of CF parameters*

$$\{\tilde{\gamma}_x = \kappa_0 + \xi_0, \tilde{\gamma}_y = \lambda_0 + \eta_0, \phi_0, \theta_0, \psi_0\}, \quad (4)$$

where the first two quantities denote the components (entire and fractionary respectively) of the *translation vector* from O to Γ_{00} , while the last three denote the Euler angles relating the CF axes to the LF axes.

Unfortunately, the solutions (4) show a strong D_M dependence [11, 12]. We are therefore obliged to devise alternative validation criteria allowing us to infer whether among the $M_{max} + 1$ areas D_M there is one showing small enough residual artifacts. Our analysis [11, 12] showed that a dozen of validation criteria have to be used to pick the most reliable CF solution. In particular, the alternative definition of Γ_{00} as *centre of symmetry* of \widetilde{D}_M and as *centre of gravity* of \widetilde{D}_M singled out the area D_0 as being the least affected by artifacts.

4.1.3 Statistical noise smoothing and background removal

A. Statistical noise smoothing. The occurrence of Umklapp components, with a rapid decay of the useful signal towards the histogram borders

(Sec. 4.1.1, item #2) suggests an off-line analysis over the various $M_{max} + 1$ areas D_M , Eq. (1). Thus, at fixed D_M , a local *window least squares* (WLS) statistical noise smoothing will be done at bins inside D_M only (the *central bins of the histogram*), while it will be skipped at the bins outside D_M (the *border bins of the histogram*).

The most convenient shape of the *smoothing window*, $C_r(K, L)$, around the (K, L) -th central bin satisfies the following requirements [10]: $C_r(K, L)$ is centred at (K, L) site; it consists of an *integer number of bins* (see Sec. 4.1.1, item #4); in the limit of an in-plane *continuous* point distribution, $C_r(K, L)$ is a *circular surface* around the point of coordinates (K, L) .

As a consequence, to perform statistical noise smoothing, we draw around *each* (K, L) -th central bin a *smoothing window* $C_r(K, L)$ of *quasi-circular shape* which includes inside it all the bins the centres (κ, λ) of which satisfy

$$(\kappa - K)^2 + (\lambda - L)^2 \leq (2r + 1)^2/4, \quad (5)$$

where the *free parameter* r is the *window radial parameter* (WRP).

To accommodate both the data discretization into bins and the possibility to predict noise-free values *inside the bins*, the approximating space of noise-free data is spanned by a basis set of polynomials of continuous variables, $P_m(x, y)$, orthogonal over $C_r(K, L)$.

Within each smoothing window (5), *constant bin weights*, $\sigma_{K+\kappa, L+\lambda} = \sigma_{KL}$, may be assumed [10]. This results in a *constant weight WLS smoothing formula* of radial parameter r (CW-WLS(r)). At the fractionary coordinates (ξ, η) , inside the (K, L) -th bin, the CW-WLS(r) yields a value [10, 13]

$$s_{K+\xi, L+\eta} = \sum_{K+k, L+l \in C_r(K, L)} h_{K+k, L+l} G(\xi, \eta; k, l), \quad (6)$$

which defines the (K, L) -th element of the smoothed 2D-ACAR histogram S .

Since the values of ξ and η may be *arbitrary* within the range $[-0.5, 0.5]$, the discretization of the S histogram may be *different* from that of the raw histogram H . Discretization steps a_D^x and a_D^y may be tailored which are *rational fractions* of the 1BZ edges p_x and p_y respectively, allowing straightforward exploitation of the space group properties of the crystal lattice [11, 13].

There is a unique value of the WRP r in Eq. (5), which selects the *best function within the admissible class* spanned by the basis polynomials. In [9, 10, 11], this parameter was only roughly optimized: it was kept constant inside a given M -Umklapp manifold, but different values were used at various M -Umklapp components. Later on it was shown [13] that the *study of the distribution of the signs of the residuals* of the smoothed data allows the derivation of *optimal WRP values at each individual bin*.

B. Background removal. Except for the tiny fraction of conduction electrons, the contributions to a 2D-ACAR histogram measured in a high- T_c superconductor (Sec. 4.1.1, item #3), form a useless background, removed so far by three kinds of methods:

- (i) Subtraction from the smoothed histogram S of the same histogram rotated by 90 degrees. This procedure is very easy to use. It was able to resolve 2- and 3-Umklapp components of the Fermi surface ridge [27, 10, 9].
- (ii) Computation of the spectrum component which is radially symmetric with respect to Γ_{00p_z} , as an inner envelopatrix of S , and its subtraction to get the anisotropic part of the spectrum. This approach, which is much more difficult to implement, allows signal resolution inside the central region D_0 , characterized by the highest signal to noise ratio [11].
- (iii) In an ideal single crystal, the 2D-ACAR resolved Fermi surface jumps yield specific jumps in the distribution of the optimally adapted to the data WRPs, Eq. (5). In a real crystal, the smearing of the derived WRP optimal values, which originates from positron annihilations with electrons at crystal imperfections, is ruled out by median smoothing of the obtained distribution, over symmetry defined stars of bins. We are thus left with a subtractionless procedure of resolving the Fermi surface jumps [13].

4.2 THE TWO BAND SINGLET-HOLE HUBBARD MODEL

The two band asymmetric singlet-hole Hubbard model developed by Plakida for the description of the high temperature superconductivity in cuprates was convincingly demonstrated to provide an adequate frame for the consistent description of the normal state of a high- T_c superconductor [22].

There was good hope that the Green function (GF) equation of motion method using a fermionic GF within a two step approach to the solution: (i) GF solution in the molecular field approximation (MFA), and (ii) GF solution of the Dyson equation with self-energy corrections included, would be the right way to the solution of the superconducting state.

- **The MFA solution**

Our investigations [23] showed that the MFA solution *cannot* be recovered using the standard approach consisting in the **decoupling** of

the three-particle anomalous correlation functions. The surprising result we have got was that both the two-particle anomalous correlation functions and the decoupled three-particle correlation functions *vanish*, hence, apparently there was not superconducting pairing within MFA.

The right way to the MFA solution involved the development of an equation of motion method for a bosonic GF which made possible the separation of exponentially small two-particle terms from significant ones *without decoupling the three-particle anomalous correlation functions*.

The final result pointed towards the existence of an *exchange $d_{x^2-y^2}$ pairing due to interband hopping*. In this way, the necessary connection (correspondence principle) with the simpler t - J model was established.

- **Beyond MFA: the weak coupling approximation**

The insight got from the solution of the Dyson equation in the weak coupling approximation [23] can be summarized as follows:

- Besides the exchange pairing mechanism, there is also present a *spin-fluctuation pairing mechanism* (due to intra-band hopping) which contributes T_c enhancement.
- The spin-fluctuation contribution is *weaker* than the exchange contribution (hence the MFA approach is consistent!).
- The variation of the spin-fluctuation energy gap inside the first Brillouin zone is canceled to a large extent by geometric structure factors and this explains why the exchange pairing is dominant.

- **Beyond MFA: the strong coupling case**

The strong coupling case (which is the physical case) is an *open question*. There are two possible alternatives: either the weak coupling result *is confirmed*, or a perverse contribution cancellation may rule it out. (In view of precedents encountered in the frame of the many-body theory, the later possibility is not a rhetoric question only!).

The attempt to attack this physical case was hindered by the finding, got from extensive numerical simulations, that the output accuracy, diagnosed by the existing quadrature algorithms to be *reliable* for the *parametric integrals* of interest, in fact *fails badly*.

A way towards reliable output was devised [24]. It is considered in the next section.

4.3 NUMERICAL INTEGRATION

In Sec. 3, two critical reliability requirements of the quadrature algorithms, related respectively to the first and the second terms of the couple $\{s, e\}$, Sec. 2.1, of a numerical solution have been noticed:

- the recovery of the value of the Riemann integral of interest within a class of quadrature sums under an infinitesimally small norm of the discretization of the integration domain performed by the mesh of the quadrature knots, and
- the choice of the correct algorithm branch within the decision process of the automatic adaptive quadrature.

There is an important physical motivation why further consideration of the reliability of the numerical integration is necessary. Many physical models currently under study (like, e.g., the two-band singlet-hole Hubbard model of cuprate superconductors [22], [23], discussed in Sec. 4.2, the $U(1) \times SU(2)$ gauge theory model of underdoped cuprate superconductors [32], [33], and a model of nuclear fission [34]) are characterized by two combined features. First, the properties of the physical system critically depend on the variations of one or more specific parameters (like, e.g., the doping parameter in cuprates). Second, the observables are obtained as parametric integrals which cannot be solved analytically. As a consequence, deep understanding of the predictions of the models needs the exploration of the values of the observables over a large range of the variable parameters.

As usual, to solve the occurring parametric integrals, recourse is made to existing library codes of automatic adaptive quadrature which may fail badly without providing any hint in this respect. This circumstance comes from the fact that the existing algorithms for the numerical integration of real valued functions (see, e.g., [35] for details on the available algorithms and a recent review of numerical quadrature) are tailored for specific classes of integrands, with limited possibilities to solve simultaneously families of integrals falling in different classes.

Two ways are to be explored to enhance the output reliability: the *extension of the reliability range of the quadrature sums* and the *improvement of the reliability diagnostics of the quadrature error estimates*.

4.3.1 Extension of the reliability range of the quadrature sums

The simplest Riemann integral needing numerical solution can be written as

$$I \equiv I[a, b]F = \int_a^b F(x)dx, \quad -\infty < a < b < \infty, \quad (7)$$

where the *integrand* $F(x)$ is assumed to be *continuous almost everywhere* on $[a, b]$, such that (7) exists and is finite.

The most performing quadrature sums for the numerical solution of (7) are based on the approximation of the integrand $F(x)$ by an *interpolatory polynomial* spanned by a system of orthogonal elementary basis polynomials which define a *Chebyshev system*. This is equivalent [36] to the requirement of getting a quadrature formula able to solve exactly the series of integrals (7) for an as large number of terms as possible within the set of integrands belonging to the fundamental power series

$$\{1, x, x^2, \dots\} . \quad (8)$$

The Gauss-Kronrod quadrature [37] and the Clenshaw-Curtis quadrature [38], provide the best available quadrature algorithms expressed as *local quadrature rules* $\{q, e\}$.

Both kinds of quadrature rules obtained at prescribed degrees of the interpolatory polynomials approximating $F(x)$ are characterized by specific *reliability ranges* the measure of which is the *maximal length* $h = |b - a|$ of the integration domain $[a, b]$ over which the discretizations secured by the corresponding sets of quadrature knots result in numerical solutions of requested accuracy.

While for *smooth slowly varying* integrands $F(x)$ satisfactory approximate solutions can be obtained for large enough lengths h , the value of this parameter becomes exceedingly small for integrals (7) of the form

$$I \equiv I^g[a, b]f = \int_a^b f(x)g(x)dx , \quad -\infty < a < b < \infty . \quad (9)$$

where $f(x)$ is still called *integrand*, while the factor $g(x)$, called *weight function*, is an analytically integrable function which absorbs a *difficult part* of the integrand (e.g., an oscillatory or a singular factor).

The way of increasing the range of the parameter h at which the numerical solution lies within the accuracy prescribed at the input consists in the use of a polynomial approximation $P_n(x)$ for the factor $f(x)$ only and the derivation of convenient expressions for the integral of the product $P_n(x)g(x)$. Here we consider two kinds of generalizations obtained for oscillatory or hyperbolic weight factors, when $g(x)$ is given by one of the following four expressions:

$$g(x) = \begin{cases} \cos(\omega x + \delta), \\ \sin(\omega x + \delta), \\ \cosh(\omega x + \delta), \\ \sinh(\omega x + \delta). \end{cases} \quad (10)$$

A. Clenshaw-Curtis quadrature. The first generalization of the Clenshaw-Curtis quadrature to integrals (9) with trigonometric weight factors $\cos(\omega x)$ or $\sin(\omega x)$ was thoroughly described in QUADPACK [37]. There, the quadrature weights associated to the product $P_n(x)g(x)$ were derived as numerical solutions of a difference system.

Subsequently, it was shown [14] that, for all the four weight functions $g(x)$ (10) it is possible to express the quadrature weights of the coefficients of the Chebyshev series expansion of $f(x)$ as well-conditioned linear combinations of the basis set of hypergeometric functions

$$\{ {}_0F_1(k - 1/2; \eta\lambda^2/4) \mid k = 2, 3, \dots, n + 2 \}, \quad (11)$$

where $\eta = -1$ for trigonometric weight functions, $\eta = 1$ for hyperbolic weight functions, while $\lambda = |\omega h|/2$.

In this way, the numerical difficulties associated to the extension of the Clenshaw-Curtis quadrature to oscillatory functions were reduced to those associated to accurate computation of basis sets of interest of hypergeometric functions (11). Ways to compute such sets to machine accuracy were devised [14]. The reliability ranges of such Clenshaw-Curtis quadrature sums are *infinite* with respect to the frequency parameter ω (hence an *absolute optimum* was reached). With respect to the extension h of the integration domain $[a, b]$, they are uniquely determined by the accuracy of the n -th degree Chebyshev series expansion of the integrand $f(x)$.

Quadrature error estimates of increased reliability were also derived [14].

B. Simpson quadrature. The Simpson quadrature sum for the approximate computation of (7)

$$q_S = \frac{b-a}{6} [F(a) + 4F(c) + F(b)], \quad c = \frac{b+a}{2}, \quad (12)$$

has acquired large popularity due to its property of showing $\mathcal{O}(h^4)$ accuracy under the computation of three integrand values only.

Under the occurrence of a factorization (9) with the weight function $g(x)$ running over one of the four factors listed in Eq. (10), the reliability range of the Simpson quadrature formula (12) severely decreases with the increase of the absolute value $|\omega|$ of the frequency parameter of $g(x)$.

A way of extending the reliability range of the Simpson quadrature sums at frequency parameters $\omega \neq 0$ uses the so called *exponential fitting* approach [39], [40]. This essentially follows a two-step Rayleigh-Ritz procedure [15]. At the first step, it is assumed that a quadrature formula of the form (12) holds with ω -dependent coefficients multiplying the three integrand values

$F(a)$, $F(c)$, and $F(b)$. At the second step, the coefficients are fixed asking the quadrature formula to be exact for a suitably chosen set of products of power and trigonometric polynomials instead of the fundamental power series (8).

This Rayleigh-Ritz procedure extends considerably the ω -dependent reliability range of the exponentially fitted Simpson quadrature formula as compared to that of the classical formula (12). However, the exponential fitting does not reach an absolute optimum of the reliability range with respect to ω .

Such an absolute optimum is reached [15] asking for the derivation of a Simpson-like quadrature formula for the explicitly factorized integral (9) under the use of Chebyshev series expansion of the factor $f(x)$ only. Of course, such a formula is a particular case of the general Clenshaw-Curtis quadrature formulas derived in [14].

4.3.2 Improving the reliability diagnostics of the quadrature error estimates

The output of a quadrature rule is *reliable* provided it is able to distinguish between a quadrature sum which *stabilized as Riemann sum* and a quadrature sum trying to use an insufficiently resolved integrand structure. In the former case, the error estimate e of the computed quadrature sum q is *bound from below* by the actual (unknown) quadrature error. In the latter case, the error estimate e might *underestimate* the actual quadrature error, without being able to set a correct diagnostic of the quadrature rule output.

Since the number of diagnostic failures gets severely increased in the case of parametric integrals, we recently undertook studies able to results in inferences approaching the theoretical 100% rate of success [16], [24].

The general picture offered by the numerical evidence on the solution of parametric integrals points towards the existence of a limited range of parameter values where the local quadrature sum q provides accurate solution of the integral of interest, whereas for other parameter values the quadrature sum q is inaccurate. Over the range of accurate q outputs, the existing quadrature error estimators provide outputs e which, in most cases, *grossly overestimate* the actual quadrature error, whence the need of supplementary range subdivisions and overcomputing to meet the input precision requests. However, over the range of inaccurate q outputs, the heuristics implemented in the local error estimators may result in spurious outputs quoted as reliable, hence the impossibility to detect such cases by means of the existing library codes.

The cornerstone of an analysis able to reconcile these two contradictory

aspects is the derivation of reliability criteria for the *validation of the local error estimate* e associated to a local quadrature sum q based on the study of the *profile of the integrand at the set of quadrature knots* entering the expression of q .

The basic idea is that an unreliable estimate of e might originate either in the *insufficient resolution* of the integrand profile, or in the presence of *difficult isolated points* (integrable singularities, turning points, jumps) which result in slow convergence. The occurrence of each kind of difficulty can be evidenced by means of specific consistency criteria asking for the fulfillment of requirements following from quite general considerations: the very definition of the Riemann integral, the fundamental properties of the basis polynomials which span the approximating linear space where the interpolatory polynomial of the quadrature rule is defined, the properties of the continuous functions at or near their extremal points, and the smoothness properties of the continuous functions inside their monotonicity subranges.

If the integrand is well-conditioned but its profile is insufficiently resolved at the current set of quadrature knots, repeated subdivision of the integration range eventually results in the fulfillment of all the reliability constraints. A genuine difficult integrand point, however, recurs under repeated subrange subdivisions. Therefore, repeated analysis of the integrand profile under subrange subdivision ultimately results in the *diagnostics stability under iteration*. This is the point where the general control routine of an automatic quadrature rule can take safe decisions concerning the best way to continue the solution refinement or to decide that the integral was solved within the input accuracy specifications.

Acknowledgments

The acquaintance with the Unix operating system and the work abroad at ICTP Trieste and at the University of Geneva during the eighties were made possible by the strong and constant support received from Professor Marin Ivaşcu, then a General Director of IFIN-HH.

References

- [1] Gh. Adam, "Experiments with general purpose visualization software on a Unix workstation", ICTP Trieste Internal Report IC/95/318.
- [2] J. Glenn Brookshear, *Computer science – An overview*, fifth ed., Addison Wesley Longman, 1997.
- [3] David Loshin, *Efficient memory programming*, Mc Graw-Hill, New York, 1999.

-
- [4] R. W. Hamming, *Numerical Methods for Scientists and Engineers*, 2-nd ed. Mc Graw-Hill, New York, 1973.
- [5] B.W. Boehm, J.R. Brown, H. Kaspar, M. Lipow, G.J. Macleod, M.J. Meritt, *Characteristics of software quality*, North Holland, Amsterdam, 1978.
- [6] M. Peter, W. Klose, Gh. Adam, P. Entel, Ewa Kudla, *Helv. Phys. Acta* **47**, 807–832 (1974).
M. Peter, Gh. Adam, *Rev. Roum. Phys.* **21**, 385–399 (1976).
- [7] L. Hoffmann, W. Sadowski, A. Shukla, Gh. Adam, B. Barbiellini, M. Peter, *J. Phys. Chem. Solids* **52**, 1551–1556 (1991).
- [8] L. Hoffmann, A. A. Manuel, M. Peter, E. Walker, M. Gauthier, A. Shukla, B. Barbiellini, S. Massidda, Gh. Adam, S. Adam, W.N. Hardy, Ruixing Liang, *Phys. Rev. Lett.* **71**, 4047–4050 (1993).
- [9] Gh. Adam, S. Adam, B. Barbiellini, L. Hoffmann, A. A. Manuel, M. Peter, S. Massidda, *Solid State Comm.* **88**, 739–742 (1993).
- [10] Gh. Adam, S. Adam, B. Barbiellini, L. Hoffmann, A. A. Manuel, M. Peter, *Nucl. Instr. Meth. in Phys. Res.* **A337**, 188–203 (1993).
- [11] Gh. Adam, S. Adam, *Int. J. Mod. Phys. B* **9**, 3667–3687 (1995).
- [12] Gh. Adam, S. Adam, *Romanian J. Phys* **42** No.9–10, 689–695 (1997); *ibid.*, **43** No.1–2, 75–88 (1998); *ibid.*, **43** No.1–2, 89–104 (1998).
- [13] Gh. Adam, S. Adam, *Comp. Phys. Comm.* **120**, 215–221 (1999).
- [14] Gh. Adam, A. Nobile, *IMA J. Numer. Analysis* **11** 271–296 (1991).
- [15] Gh. Adam, S. Adam, *Comp. Phys. Comm.* **125** (no. 1–3), 127–141 (2000); *ibid.*, **134** (no. 2), 269–272 (2001).
- [16] Gh. Adam, S. Adam, *Comp. Phys. Comm.* **135** (no. 3), 261–277 (2001).
- [17] Gh. Adam, L. Gr. Ixaru, *Rev. Roum. Phys.* **20**, 17–28 (1975).
Gh. Adam, L. Gr. Ixaru, A. Corciovei, *J. Comp. Phys.* **22**, 1–33 (1976).
Gh. Adam, *Rev. Roum. Phys.* **24**, 951–969 (1979).
Gh. Adam, *Rev. Roum. Phys.* **33**, 1239–1265 (1988); *ibid.*, **33**, 1267–1293 (1988).
- [18] S. Adam, Gh. Adam, A. Corciovei, *Rev. Roum. Phys.* **22**, 39–52 (1977).
S. Adam, Gh. Adam, A. Corciovei, *physica status solidi (b)* **105**, 85–92 (1981); *ibid.*, **(b)114**, 85–93 (1982); *ibid.*, **(b)129**, 763–774 (1985).

- [19] S. Adam, Gh. Adam, E. Burzo, *J. Magn. Magn. Mat.* **61**, 260–266 (1986);
E. Burzo, Gh. Adam, S. Adam, W. E. Wallace, *Rev. Roum. Phys.* **33**,
457–461 (1988).
- [20] Gh. Adam, S. Adam, G. M. Gavrilenco, D. Mihalache, V. K. Fedyanin,
preprint OIYal–Dubna **P17–80–748**, (1980);
Gh. Adam, S. Adam, G. M. Gavrilenco, D. Mihalache, V. K. Fedyanin,
preprint OIYal–Dubna **P17–82–868**, (1982);
Gh. Adam, S. Adam, V. K. Fedyanin, G. M. Gavrilenco, D. Mihalache,
preprint OIYal–Dubna **P17–83–291**, (1983).
- [21] Gh. Adam, S. Adam, V. K. Fedyanin, *Rev. Roum. Phys.* **32**, 769–783
(1987).
- [22] N.M. Plakida, R. Hayn, J.-L. Richard, *Phys. Rev. B* **51**, 16599 (1995).
N.M. Plakida, *Physica C* **282–287**, 1737 (1997).
- [23] N.M. Plakida, L. Anton, S. Adam, Gh. Adam, *JINR Dubna Preprint*,
E-17-2001-59;
N.M. Plakida, L. Anton, S. Adam, Gh. Adam, [http://arXiv.org/cond-
mat/0104234](http://arXiv.org/cond-mat/0104234);
N.M. Plakida, L. Anton, S. Adam, Gh. Adam, in *New Trends in Su-
perconductivity*, NATO Science Series, vol. 67, J.F. Annett and S. Kru-
chinin, Eds., Kluwer Academic Publishers, Dordrecht, 2002, pp. 29–38;
N.M. Plakida, L. Anton, S. Adam, Gh. Adam, *ZhETF* **124** No. 1 (7)
(2003), in press.
- [24] Gh. Adam, S. Adam, N.M. Plakida: "Reliability conditions on quadra-
ture algorithms", *JINR-Dubna Preprint* E17-2002-205.
Extended version available at: <http://arXiv.org/abs/cs.NA/0303004>,
at <http://www.mathpreprints.com/math/Preprint/adamg/20030415/1>
and *Comp. Phys. Comm.* **154** (no. 1) 49–64 (2003).
- [25] P.E. Bisson, P. Descouts, A. Dupanloup, A.A. Manuel, E. Perreard,
M. Peter and R. Sachot, *Helv. Phys. Acta* **55**, 100 (1982).
- [26] S. Berko in *Positron Solid State Physics, Proc. of the Internat'l School
"E. Fermi", Course 83*, eds. W. Brandt and A. Dupasquier (North
Holland, New York, 1983) pp. 64–145. Reprinted in *Positron Studies
of Solids, Surfaces and Atoms*, eds. A.P. Mills, Jr., W.S. Crane and
K.F. Canter (World Scientific, Singapore, 1986) pp. 246–327.
- [27] H. Haghighi, J.H. Kaiser, S. Rayner, R.N. West, J.Z. Liu, R. Shelton,
R.H. Howell, F. Solal and M.J. Fluss, *Phys. Rev. Lett.* **67**, 382 (1991).

-
- [28] L.P. Chan, K.G. Lynn and D.R. Harshman, *Mod. Phys. Lett. B* **6**, 617 (1992).
- [29] L.C. Smedskjaer, A. Bansil, U. Welp, Y. Fang and K.G. Bailey, *Physica C* **192**, 259 (1992).
- [30] R. Pankaluoto, A. Bansil, L.C. Smedskjaer and P.E. Mijnders, *Phys. Rev. B* **50**, 6408 (1994).
- [31] L.C. Smedskjaer and D.G. Legnini, *Nucl. Instr. and Meth. A* **292**, 487 (1990).
- [32] P.A. Marchetti, Zhao-Bin Su, and Lu Yu, *Phys. Rev. B* **58**, 5808–5824 (1998).
- [33] P.A. Marchetti, Jian-Hui Dai, Zhao-Bin Su, and Lu Yu, *J. Phys.: Cond. Matter*, **12**, L329–L336 (2000).
- [34] A. Săndulescu, F. Cârstoiu, Ş. Mişicu, A. Florescu, A.V. Ramayya, J.H. Hamilton, J.K. Hwang, W. Greiner, *Phys. Rev. C* **57**, 2321 (1998).
- [35] A.R. Krommer and C.W. Ueberhuber. *Computational Integration*, SIAM, Philadelphia, 1998.
- [36] P.J. Davis and P. Rabinowitz, *Methods of Numerical Integration*, Second edition, Academic Press, Orlando (Fla), USA, 1984.
- [37] R. Piessens, E. deDoncker-Kapenga, C.W. Ueberhuber, and D.K. Ka-haner, *QUADPACK, a subroutine package for automatic integration*, Springer Verlag, Berlin, 1983.
- [38] C.W. Clenshaw, A.R. Curtis, *Numer. Math.* **2**, 197-205 (1960).
- [39] U.T. Ehrenmark, *J. Comp. and Appl. Math.* **21**, 87–99 (1988).
- [40] L.Gr. Ixaru, *Computer Phys. Commun.* **105**, 1–19 (1997).